Research Report

Global Sensitivity Analysis of OnGuard Models Identifies Key Hubs for Transport Interaction in Stomatal Dynamics[1][CC-BY]

Silvere Vialet-Chabrand[2], Adrian Hills[2], Yizhou Wang[2,3], Howard Griffiths, Virgilio L. Lew, Tracy Lawson, Michael R. Blatt*, and Simon Rogers

Biological Sciences, University of Essex, Colchester CO4 3SQ, United Kingdom (S.V.-C., T.L.); Laboratory of Plant Physiology and Biophysics (A.H., Y.W., M.R.B.) and Computing Science (S.R.), University of Glasgow, Glasgow G12 8QQ, United Kingdom; Plant Sciences, University of Cambridge, Cambridge CB2 3EA, United Kingdom (H.G); and Physiological Laboratory, University of Cambridge, Cambridge CB2 3EG, United Kingdom (V.L.L.)

ORCID IDs: 0000-0002-4705-0756 (A.H.); 0000-0002-2188-383X (Y.W.); 0000-0002-0554-2701 (V.L.L.); 0000-0002-4073-7221 (T.L.); 0000-0003-1361-4645 (M.R.B.); 0000-0003-3578-4477 (S.R.).

The physical requirement for charge to balance across biological membranes means that the transmembrane transport of each ionic species is interrelated, and manipulating solute flux through any one transporter will affect other transporters at the same membrane, often with unforeseen consequences. The OnGuard systems modeling platform has helped to resolve the mechanics of stomatal movements, uncovering previously unexpected behaviors of stomata. To date, however, the manual approach to exploring model parameter space has captured little formal information about the emergent connections between parameters that define the most interesting properties of the system as a whole. Here, we introduce global sensitivity analysis to identify interacting parameters affecting a number of outputs commonly accessed in experiments in Arabidopsis (*Arabidopsis thaliana*). The analysis highlights synergies between transporters affecting the balance between Ca^{2+} sequestration and Ca^{2+} release pathways, notably those associated with internal Ca^{2+} stores and their turnover. Other, unexpected synergies appear, including with the plasma membrane anion channels and H^+-ATPase and with the tonoplast TPK K^+ channel. These emergent synergies, and the core hubs of interaction that they define, identify subsets of transporters associated with free cytosolic Ca^{2+} concentration that represent key targets to enhance plant performance in the future. They also highlight the importance of interactions between the voltage regulation of the plasma membrane and tonoplast in coordinating transport between the different cellular compartments.

Stomata form the major pathway for CO_2 entry across the leaf epidermis for photosynthesis and for water loss by transpiration from the leaf tissues. Pairs of guard cells surround the stomatal pore and regulate the aperture. These cells balance the demand for CO_2 with that for water conservation. Guard cells expand and contract to open and close the pore. They take up and lose solutes, notably K^+ and Cl^-, which, together with the synthesis and metabolism of organic solutes, especially malate, provide the osmotic driving force for these changes in aperture (Kim et al., 2010; Roelfsema and Hedrich, 2010; Lawson and Blatt, 2014). Thus, membrane transport comprises the principal set of effectors of a regulatory network that ensures the homeostatic control of the guard cell for stomatal aperture.

Environmental signals, notably light, CO_2, water availability, and the hormone abscisic acid, affect this network, modulating transport and solute accumulation. Research at the cellular and molecular levels has focused on these inputs and their contributions to stomatal movements. A large body of work has highlighted Ca^{2+}-independent and Ca^{2+}-dependent signaling, the latter including elevations in free cytosolic Ca^{2+} concentration ($[Ca^{2+}]_i$), protein kinase and phosphatase activities, which inactivate inward-rectifying K^+ channels and activate Cl^- (anion) channels, as well as the changes in cytosolic pH that promote the outward-rectifying K^+ channels and solute loss (Keller et al., 1989; Blatt et al., 1990; Thiel et al., 1992; Lemtiri-Chlieh

[1] This work was supported by the Biotechnology and Biological Sciences Research Council (grant nos. BB/L019205/1 and BB/M001601/1 to M.R.B., grant no. BB/L001276/1 to M.R.B. and S.R., and grant no. BB/I001187/1 to H.G. and T.L.).

[2] These authors contributed equally to the article.

[3] Present address: Biology, Washington University, Campus Box 1037, One Brookings Drive, St. Louis, MO 63130.

* Address correspondence to michael.blatt@glasgow.ac.uk.

The author responsible for distribution of materials integral to the findings presented in this article in accordance with the policy described in the Instructions for Authors (www.plantphysiol.org) is: Michael R. Blatt (michael.blatt@glasgow.ac.uk).

S.V.-C. and S.R. developed the Sobol analysis routines with support from A.H. and carried out interaction analyses; A.H., M.R.B., and V.L.L. developed OnGuard routines; Y.W., H.G., V.L.L., M.R.B., and T.L. contributed to discussions of output and its interpretation; S.V.-C., S.R., and M.R.B. wrote the article with support from all authors.

www.plantphysiol.org/cgi/doi/10.1104/pp.17.00170

and MacRobbie, 1994; Grabov and Blatt, 1998, 1999; for review, see Blatt, 2000; Hetherington and Brownlee, 2004; Kim et al., 2010; Lawson and Blatt, 2014; Jezek and Blatt, 2017).

Despite this extensive body of knowledge about the individual transporters and their regulation, relating the transport capacity of guard cells to stomatal movements in quantitative mechanistic terms poses a number of difficulties. Most important, the physical requirement in transport for charge to balance across each membrane means that the transport of any one ionic species is necessarily joined to that of all others across the same membrane (Jezek and Blatt, 2017). As a result, the capacity for flux through most transporters is rarely limiting, especially through the individual ion channels that facilitate K^+, Cl^-, and malate flux. Instead, transport is generally limited by the balance in charge flux across the plasma and tonoplast membranes. As a corollary, manipulating solute flux through any one transporter inevitably affects this balance in transport and, thereby, directly affects other transporters at the same membrane, often with unforeseen consequences.

Systems modeling offers one approach for overcoming these difficulties to quantify the mechanics of stomatal movements and to predict and interpret the effects of experimental manipulations. It enables the detailed knowledge available for the individual transporters to be reconstructed within the physiological framework of the cell, fully constrained by fundamental physical laws and the known kinetic relationships, ligand binding, and related regulatory properties for each transporter. The development of the OnGuard platform for modeling guard cells (Chen et al., 2012; Hills et al., 2012; freely available at www.psrg.org.uk) has proven most successful to date, demonstrating true predictive power in uncovering previously unexpected and emergent behaviors of stomata (Wang et al., 2012, 2014a; Blatt et al., 2014; Minguet-Parramona et al., 2016).

Despite these successes, resolving models with the OnGuard platform to date has required manual exploration with over 200 parameters that define the characteristics of the dominant ion transporters and organic solute metabolism. Roughly 85% of these parameters are known experimentally to within a factor of 3, and half of these are known accurately to within a margin of 5% to 10% of the parameter value. Nonetheless, refining OnGuard models has remained an arduous task, often demanding many weeks to explore the parameter space across each selection of experimental variables. Furthermore, this process captures little formal information about the connections between subsets of parameters that determine transport, defining its most interesting characteristics that emerge from interactions within the system as a whole. We have now implemented a semiautomated approach to estimate the importance of transporters and the interactions between them in OnGuard, making use of global sensitivity analysis methods to determine the parameter subsets that, together, account for the largest proportions of variance in several model outputs that are commonly reported in experimental studies. Our findings highlight the emergent synergy inherent in transport and the several hubs of interaction between transport functions. This information is likely to help in selecting potential targets for enhancing plant performance in the future. It also demonstrates the importance of the trans-network of interactions between the plasma membrane and tonoplast that coordinates transport between the different cellular compartments.

RESULTS AND DISCUSSION

Figure 1 shows the standard Arabidopsis model outputs for stomatal aperture and $[Ca^{2+}]_i$ over the diurnal cycle with stepwise light transitions. Also shown is an exploded view of the $[Ca^{2+}]_i$ time course at the end of the daylight period and following the transition to dark when the stomata close (Chen et al., 2012; Wang et al., 2012). The oscillations in $[Ca^{2+}]_i$ are coupled to oscillations in membrane voltage of several minutes duration, with transients in $[Ca^{2+}]_i$ from values near 200 nM to maxima in excess of 1 μM. This entire sequence of oscillations is stably repeated with each diurnal cycle for all

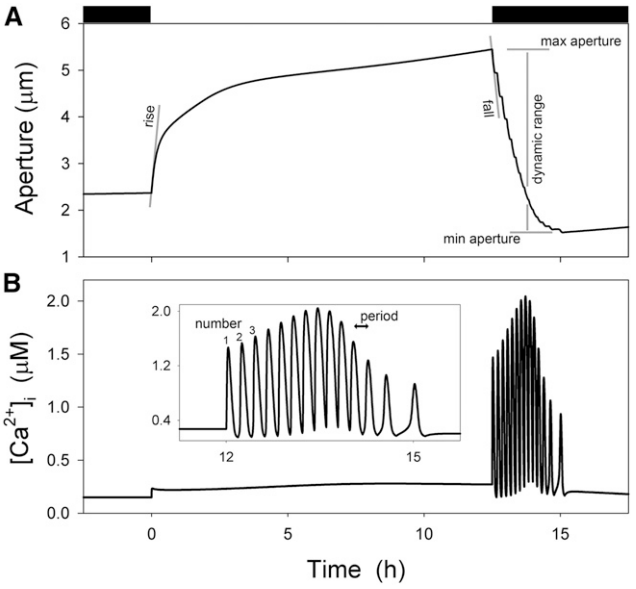

Figure 1. Macroscopic outputs of the OnGuard Arabidopsis model. Outputs resolved over a diurnal cycle with stepped transitions between dark and light (the dark period is indicated by the black bar above) and with 10 mM KCl, 1 mM $CaCl_2$, and pH 6.5 outside. The full set of model parameters and initializing variables can be found in Supplemental Appendix S1 and may be downloaded with the OnGuard software at www.psrg.org.uk. A, Model output of stomatal aperture for the diurnal period −2 to 17 h relative to the start of the diurnal cycle. Secondary parameters derived from this output and used in the Sobol analysis are indicated for the initial increase (rise) and decrease (fall) in stomatal aperture, the minimum (min) and maximum (max) apertures, and the dynamic range of the aperture. B, Model output of $[Ca^{2+}]_i$. Secondary parameters derived from this output and used in the Sobol analysis are indicated for the number of $[Ca^{2+}]_i$ oscillation cycles and the oscillation period. In the latter case, the median of the oscillation periods was used.

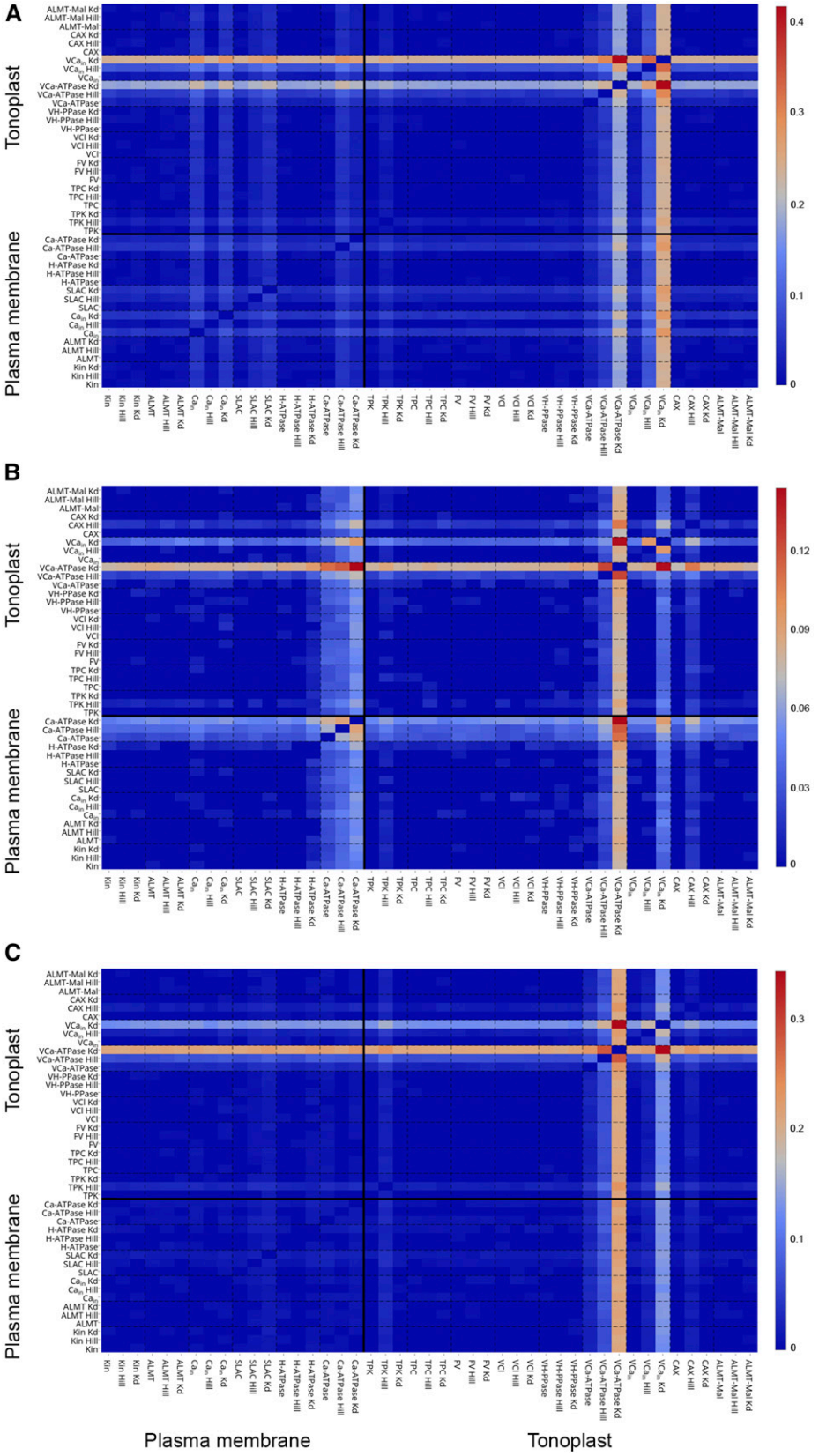

Figure 2. Sobol analysis heat map of transport parameter interactions affecting the maximum (A) and minimum (B) apertures and the aperture dynamic range (C), as defined in Figure 1, with the Sobol index scale (right). The full list of transporter identities and functions can be found in Jezek and Blatt (2017) and Hills et al. (2012). Note that the highest indices across the vertical and horizontal associated in each case with parameters for the endomembrane Ca^{2+} release channel VCa_{in} and the Ca^{2+} sequestration pump VCa-ATPase. The high indices here indicate that parameters for virtually every other transporter interact synergistically with those of the VCa_{in} and VCa-ATPase. In affecting the maximum aperture (A), this interdependence is highest for the K_d values for Ca^{2+} of the VCa_{in} and VCa-ATPase. Substantial interdependence also is seen between the K_d for Ca^{2+} of the VCa_{in} and the TPK K^+ channel of the tonoplast and parameters of the plasma membrane Ca^{2+} channel (Ca_{in}), the Cl^- channel (SLAC), and the Ca^{2+} export pump (Ca-ATPase). Note, too, that a similar set of interdependencies is seen in the aperture dynamic range (C), albeit primarily with the VCa-ATPase, and that the interdependencies affecting the minimum aperture (B) are generally of lower index values and include hubs associated with the plasma membrane Ca^{2+}-ATPase and the tonoplast Ca^{2+}/H^+ antiporter CAX.

known model parameter sets (Chen et al., 2012; Minguet-Parramona et al., 2016). The major peaks of voltage and $[Ca^{2+}]_i$ occur in antiparallel fashion and show a mean frequency of 1.9 mHz (=8.9 min) for the standard Arabidopsis parameter set (Minguet-Parramona et al., 2016), thus closely matching previously published data for $[Ca^{2+}]_i$ and voltage oscillations in these and other guard cells (Blatt and Armstrong, 1993; McAinsh et al., 1995; Grabov and Blatt, 1998; Allen et al., 2001). These oscillations also are coupled to the periodic, almost stepwise decreases in stomatal aperture evident in Figure 1. For purposes of analysis, we derived the secondary outputs, as indicated in Figure 1, that are commonly reported in experimental studies.

Global variance-based analysis with Sobol indices (Sobol, 2001) addresses problems inherent to work with model parameters that may range across many orders of magnitude and gives a detailed, high-level view of parameter interactions. The method places emphasis on the variance in parameter values and thereby obviates issues of parameter weighting. In other words, if a transporter becomes a target of interest to improve plant behavior, the variation needed will be highlighted independent of the parameter value itself. The Sobol analyses of interacting parameters for minimum and maximum stomatal aperture and the associated dynamic range are shown in Figure 2. Here, and in the following figures, the Sobol indices are shown as heat maps to highlight those transporter parameters with the strongest interdependencies: in other words, those parameters that affect the output synergistically (see "Materials and Methods"). A complete list of transporter definitions will be found in Hills et al. (2012) and Jezek and Blatt (2017), and the acronyms are summarized in Table I. We discounted trivial interactions for any one transporter, such as that between the Hill coefficient and K_d for Ca^{2+} of the endomembrane Ca^{2+} release channel (VCa_{in}), to focus on interdependencies between transporters.

A review of the maximum aperture interactions (Fig. 2A) showed a substantial dependence on the K_d for Ca^{2+} of VCa_{in} and its interactions with several other transporters, most strongly with the K_d for Ca^{2+} of the endomembrane Ca^{2+} sequestration pump VCa-ATPase but also with parameters for the plasma membrane Ca^{2+} channel Ca_{in}, the Ca-ATPase, the SLAC anion channel, and the Hill coefficient for Ca^{2+} control of the tonoplast TPK K^+ channel. These interactions yielded Sobol index values from 0.28 to 0.42, supporting the conclusion of an interdependence between these parameters and the importance of endomembrane Ca^{2+} circulation in determining the maximum aperture. They also highlight the substantial interaction between transport at the plasma membrane and tonoplast that was identified previously and associated with Ca^{2+} (Chen et al., 2012; Wang et al., 2012; Minguet-Parramona et al., 2016).

The minimum aperture (Fig. 2B) also showed an interdependence between the K_d values for Ca^{2+} of VCa_{in} and the VCa-ATPase, albeit weaker. However, nearly equivalent interdependencies also were evident for the minimum aperture between the K_d for Ca^{2+} VCa-ATPase with parameters for the plasma membrane Ca-ATPase and, to a lesser extent, with several other plasma membrane and tonoplast transporters, including the TPK K^+ channel and the CAX Ca^{2+}/H^+ antiporter. Finally, a comparison with these heat maps showed that the aperture dynamic range (Fig. 2C) was most sensitive to the interactions between the K_d values

Table I. *Transporter acronyms used in Figures 2 to 4*

Further details of the transporters, their characteristic parameters, and their inclusion in the OnGuard model can be found in Jezek and Blatt (2017) and Hills et al. (2012). Parameters examined for each transporter listed in the figures are for the transporter number (Transporter), its primary K_d (K_d), and the corresponding Hill coefficient (Hill).

Acronym	Transporter	Representative Gene Products[a]
Plasma membrane		
Ca-ATPase	Ca^{2+}-ATPase	ACA3, ACA8, ACA10
H-ATPase	H^+-ATPase	AHA1, AHA2, AHA5
SLAC	Slow-activating Cl^- channel	SLAC1
Ca_{in}	Inward-rectifying Ca^{2+} channel	Not known
ALMT	Rapid-activating Cl^- channel	ALMT12/QUAC1
K_{in}	Inward-rectifying K^+ channel	KAT1, KAT2
Tonoplast		
ALMT-malate		
CAX	H^+/Ca^{2+} antiport	CAX1, CAX3, CAX5
VCa_{in}	Ca^{2+} channel (inactivating)	Not known
VCa-ATPase	Ca^{2+}-ATPase	ACA4, ACA11
VH-PPase	H^+-pyrophosphatase	AVP1, AVP2
VCl	Vacuolar Cl^- channel	ALMT9
FV	Fast-activating K^+ channel	Not known
TPC	Tonoplast cation channel	TPC1
TPK	Tonoplast K^+ channel	TPK1, KCO3

[a]Gene product names are for Arabidopsis.

for Ca^{2+} of VCa_{in} and the VCa-ATPase, but unlike the maximum aperture, the dominant interactions otherwise were between the K_d for Ca^{2+} of the VCa_{in} with parameters of the plasma membrane Ca^{2+} channel, the SLAC anion channel, and the Ca-ATPase.

Figure 3 shows the heat maps for parameter interactions affecting the initial rates of stomatal opening and closing. The most notable interactions in stomatal opening were between parameters defining the plasma membrane Ca-ATPase and the ALMT anion channel and in stomatal closing between endomembrane VCa_{in} and the plasma membrane H-ATPase. The Sobol indices in these instances ranged between approximately 0.08 and 0.15, appreciably lower than those associated with minimum and maximum apertures. Nonetheless, these interactions highlight the importance of membrane voltage, and the transporters that are most strongly affected by its variation, in driving the rates of solute accumulation and loss (Thiel et al., 1992; Minguet-Parramona et al., 2016).

Previous work highlighted the importance in stomatal closure of oscillations in membrane voltage and $[Ca^{2+}]_i$. Minguet-Parramona et al. (2016) illustrated how the coupled oscillations of voltage and $[Ca^{2+}]_i$ accelerated stomatal closure. They demonstrated that the prevalent oscillation frequencies do not drive closure per se but are the consequence of emergent interactions between the several transporters that facilitate solute loss from the guard cells. Significantly, Minguet-Parramona et al. (2016) used the OnGuard platform to reproduce observations that oscillation frequency is subject to a range of external factors, including extracellular Ca^{2+} and K^+ concentrations (McAinsh et al., 1990; Fricker et al., 1991; Gradmann et al., 1993; Grabov and Blatt, 1999), and they predicted the dependence of oscillation frequency on transport parameters such as those defining the Ca^{2+} sensitivity of the SLAC anion channel (Chen et al., 2010; Minguet-Parramona et al., 2016).

Sobol analyses for $[Ca^{2+}]_i$ oscillation frequency and number are shown in Figure 4. As might be anticipated from this previous study of $[Ca^{2+}]_i$ oscillation structure, the analysis for oscillation frequency (Fig. 4A) showed substantial interdependencies between parameters for

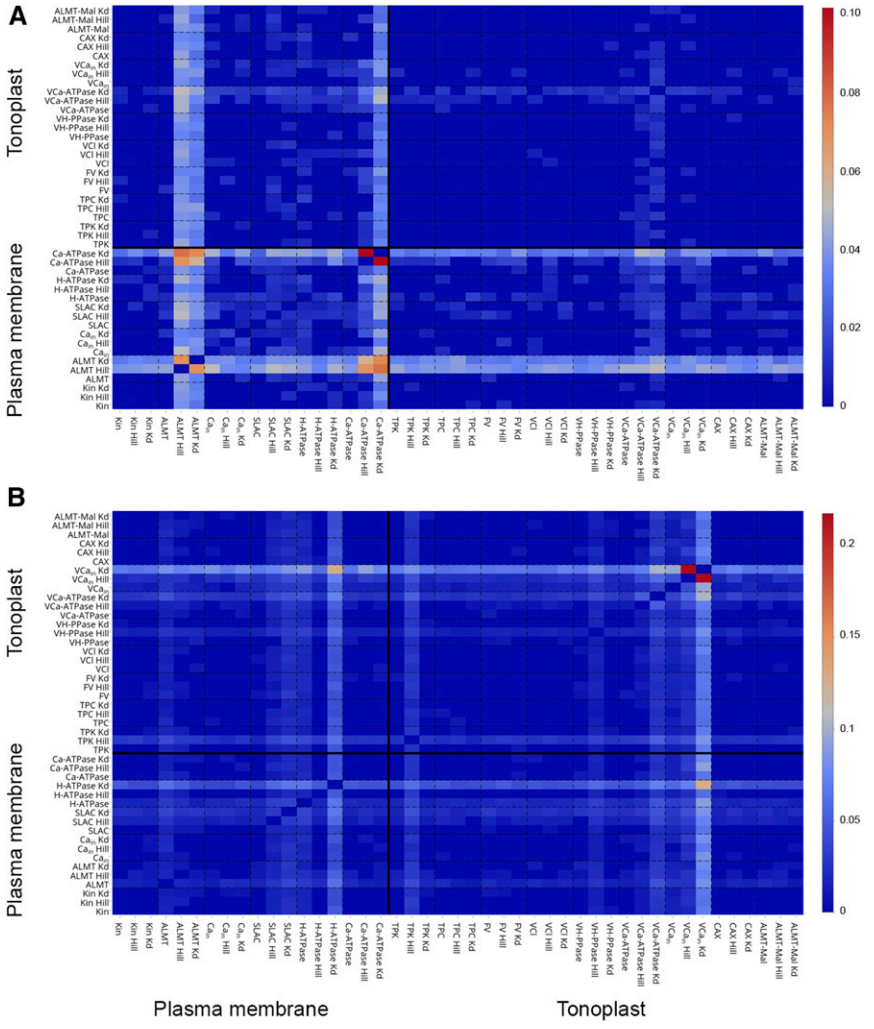

Figure 3. Sobol analysis heat map of transport parameter interactions affecting the initial rates of stomatal opening (A) and closing (B), as defined in Figure 1, with Sobol index scale (right). The full list of transporter identities and functions can be found in Jezek and Blatt (2017) and Hills et al. (2012). Note the difference in Sobol index scales. The highest indices across the vertical and horizontal are associated with the rate of closure (B) and interacting parameters for the endomembrane VCa_{in} channel and the primary plasma membrane H^+-ATPase. However, an appreciable hub also is associated with the tonoplast TPK channel. For the initial rate of stomatal opening (A), hubs of interdependence are associated with parameters for the plasma membrane Ca^{2+}-ATPase and the ALMT anion channel, which plays a key role in the control of membrane voltage and stomatal closing (Meyer et al., 2010; Wang et al., 2014a; Minguet-Parramona et al., 2016; Jezek and Blatt, 2017).

VCa_{in} and virtually every other transporter examined. The strongest interdependencies were observed with parameters for the VCa-ATPase and yielded Sobol indices near 0.2 and 0.32; however, all of the other transporter parameters yielded appreciable Sobol indices, with values around 0.16 to 0.18. Minguet-Parramona et al. (2016) also noted previously that the oscillation number was subject to the dynamic range of stomatal apertures for a given set of conditions: in other words, the number of cycles needed to transit from the open to the closed state. Thus, it was not surprising that we found weak interdependencies only, largely in the range of 0.02 to 0.04 and including the interaction between VCa_{in} and the VCa-ATPase. Unexpectedly, however, this analysis also predicted at the hub of these interactions both the VCa-ATPase and the TPK channel. Furthermore, the strongest interdependence was predicted between parameters defining TPK and VCa_{in}. This interaction is particularly noteworthy. Past studies showed that the Arabidopsis *tpk1* mutant exhibits a much reduced rate of stomatal closure, even though the K^+ content of the mutant is seemingly unaffected (Gobert et al., 2007). Given the emergent interdependence of VCa_{in} with the TPK channel, we predict that the effects of the *tpk1* mutant are mediated through their interaction with endomembrane Ca^{2+} release and their impact on $[Ca^{2+}]_i$ during stomatal closure.

Complex biological processes are defined by nonlinear relationships and are never equal to the sum of the properties of their components. New properties emerge from the interactions between components that cannot be predicted a priori, even with knowledge of the underlying processes behind each component in isolation. These so-called emergent properties (Novikoff, 1945) are amply represented by the behavior of stomata, such as in the SLAC1 Cl^- channel, nominally associated with stomatal closure, and its unexpected effects on the K^+ channel activities in stomatal opening identified through the OnGuard modeling platform. In this case, Wang et al. (2012) predicted a connection in the Arabidopsis *slac1* mutant between the Cl^- and K^+ channels at the plasma membrane that was subsequently validated experimentally. OnGuard modeling showed how *slac1* slowed K^+ uptake and stomatal opening, even though the Cl^- channel contributes directly only to solute loss and stomatal closure.

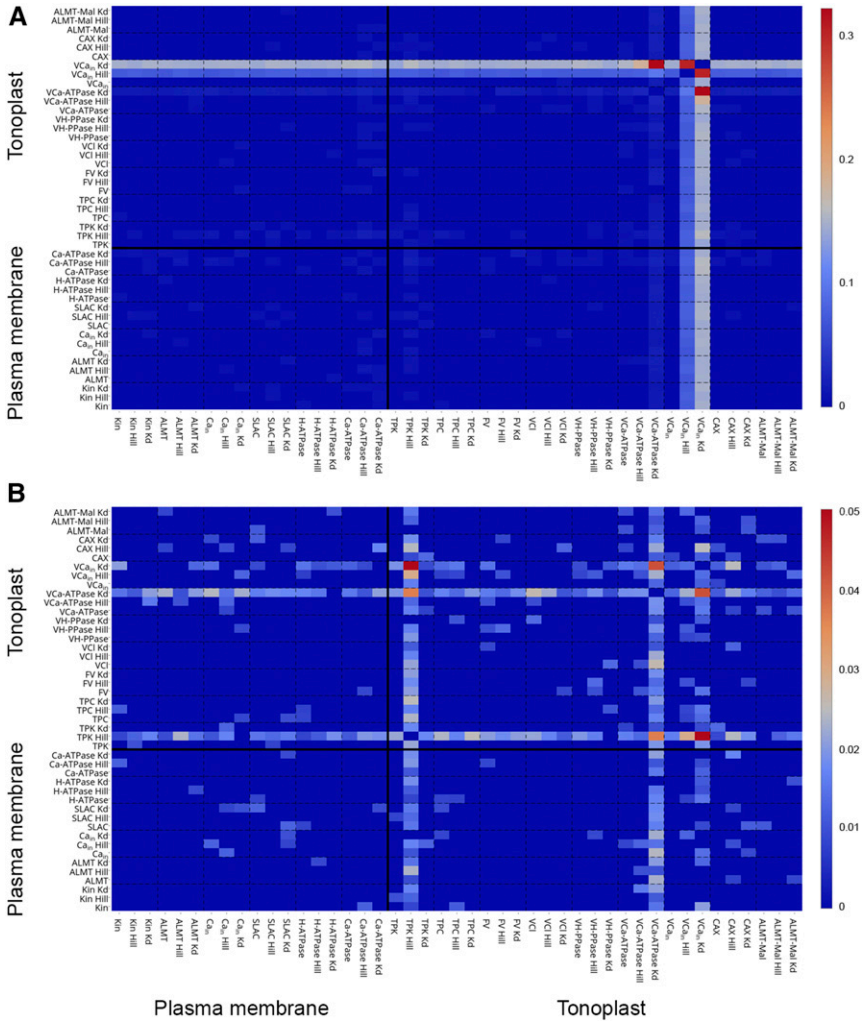

Figure 4. Sobol analysis heat map of transport parameter interactions affecting the frequency of $[Ca^{2+}]_i$ oscillations (A) and their number (B), as defined in Figure 1, with Sobol index scale (right). The full list of transporter identities and functions can be found in Jezek and Blatt (2017) and Hills et al. (2012). Note the difference in Sobol index scales. The highest indices across the vertical and horizontal are associated with the frequency of $[Ca^{2+}]_i$ oscillations (A) and interdependencies of the VCa_{in}, which serves as the primary pathway for $[Ca^{2+}]_i$ elevation. The number of $[Ca^{2+}]_i$ oscillations (B) shows a set of weak hubs of interdependence associated with the endomembrane Ca^{2+}-ATPase, VCa-ATPase, and TPK K^+ channel.

Indeed, the OnGuard platform (Chen et al., 2012; Hills et al., 2012; freely available at www.psrg.org.uk) has proven most successful to date, demonstrating true predictive power in uncovering a number of previously unexpected and emergent behaviors of guard cells (Blatt et al., 2014; Wang et al., 2014a; Minguet-Parramona et al., 2016). These studies illustrate how quantitative modeling is essential as an approach to physiology that otherwise confounds intuitive understanding and leads to misinterpretations. To date, however, reviews of the interactions inherent to this complex system of transport processes have been limited. Wang et al. (2014a) carried out a local sensitivity analysis, extracting the key macroscopic outputs, their dependencies on a selection of parameters for individual transporters, varying these parameters one at a time. Such first-order analysis, although enlightening, is not well equipped to capture global information about the interdependencies between transporters. This information is essential for any critical evaluation of how the relevant transporters are coordinated and which characteristics are most important for such coordination.

Our screen here for parameter interdependencies underscores the central importance of a number of transport interaction hubs. We selected for analysis the subset of transporters with known and direct connections to $[Ca^{2+}]_i$. These transporters comprise some 70% of the combined transport activities at the plasma membrane and tonoplast. The majority do not transport Ca^{2+} or affect $[Ca^{2+}]_i$ per se, although they respond to $[Ca^{2+}]_i$ (Jezek and Blatt, 2017). Not surprisingly, the analysis highlights interactions between transporters affecting the balance between Ca^{2+} sequestration and Ca^{2+} release pathways, notably those associated with internal Ca^{2+} stores and their turnover. The K_d values for Ca^{2+} of the endomembrane Ca^{2+} channel VCa_{in} and the VCa-ATPase are predicted to be central for interactions affecting minimum and maximum aperture (Fig. 2), the initial rate of stomatal closure (Fig. 3), and the median period and number of $[Ca^{2+}]_i$ oscillations (Fig. 4). Each of these overlapping hubs categorizes substantial synergies between parameters across virtually every transporter at both the plasma membrane and tonoplast and, thereby, underscores the intrinsic functional network engendered by transport across each membrane and also between membranes.

Other hubs of synergy surface for the ALMT anion channel associated with the initial rate of stomatal opening and for the H-ATPase associated with the initial rate of stomatal closure (Fig. 3). These were unexpected, as they are not associated directly with $[Ca^{2+}]_i$ regulation. They appear counterintuitive at first, because the ALMT channel is normally active in stomatal closure and the H-ATPase is normally active in stomatal opening. However, they make sense in light of the importance of membrane voltage in determining net solute flux (Thiel et al., 1992; Chen et al., 2012; Jezek and Blatt, 2017). The ALMT channel activates, positive-going, with a midpoint voltage near −60 mV (Dietrich and Hedrich, 1998; Meyer et al., 2010; Hills et al., 2012) and, therefore, imposes a strong, voltage-dependent brake on membrane hyperpolarization for initial solute uptake. Conversely, H-ATPase activity is key to hyperpolarizing the plasma membrane, and its activity must be suppressed for rapid stomatal closure (Merlot et al., 2007; Minguet-Parramona et al., 2016).

What is more important, therefore, is that this systematic approach offers global insights into the manner in which transport interacts to facilitate ion efflux for stomatal movements. Most useful, then, is to recognize that these emergent interactions arise through the physical requirements for the conservation of mass and charge balance in transport. Just as the oscillations in voltage and $[Ca^{2+}]_i$ described previously (Minguet-Parramona et al., 2016) simply reflect a spectrum of frequencies that emerge from the balance of intrinsic transport activities of the guard cell, so too the scope for variation within each parameter defining the various solute transporters arises from the constraints of charge coupling that are intrinsic to all transmembrane activities. In short, each hub and interdependent parameter is the by-product of the combination of characteristics that determine each transport process.

MATERIALS AND METHODS

Local sensitivity analysis is a popular tool for identifying the influence that individual parameters have on the output(s) of a model. The analysis involves repeatedly running a simulation, with a single parameter either increased or decreased, and monitoring outputs. The approach can identify parameters that have a strong influence on model behavior. Coupling between model components (in OnGuard, arising from the fundamental model construction that includes the requirement for charge balance across each membrane) means that changing parameters in isolation does not yield directly any information about the interactions between their parameters imposed by charge balance or other indirect factors such as varied ionic conditions.

To overcome these limitations, we applied Sobol sensitivity analysis (Sobol, 2001), a powerful tool for performing global sensitivity analysis. A detailed description of the procedure is beyond the scope of this article, but in essence, the analysis decomposes the variance in a particular model output into contributions from individual parameters and, crucially for this application, contributions from groups of parameters. Consider a particular model output Y, for example, maximum stomatal aperture, which is a function of a set of parameters, $X_1, X_2, \ldots, X_N$, which define several different transporters. The first-order Sobol index S_i for parameter X_i is given as

$$S_i = \frac{V_{X_i}(E_{\mathbf{X}_{-i}}(Y|X_i))}{V(Y)} = \frac{V_i}{V(Y)} \quad (1)$$

and can be interpreted as the proportion of the total variance in $Y(V(Y))$ that can be attributed to changes in X_i. In this expression, V_Z denotes the variance (with respect to Z) and $E_Z(f(Z))$ is the expected value of $f(Z)$ with respect to Z. X_{-i} is the set of all parameters excluding X_i. The larger this value, the more important X_i is considered to be with respect to the output Y. The strength of Sobol analysis is that it can be extended beyond first-order contributions (e.g. S_i) to second and higher orders. Of particular interest here are second-order contributions. In particular, S_{ij} gives the joint contribution of parameters i and j to the variance

$$S_{ij} = \frac{V_{ij}}{V(Y)} \quad (2)$$

where

$$V_{ij} = V\big(E\big(Y|X_i, X_j\big)\big) - V_i - V_j \quad (3)$$

S_{ij} gives the proportion of the total variance that can be attributed directly to interactions between these two parameters: in other words, the proportion attributed to i and j minus their individual contributions. Most important, a high

value of S_{ij} indicates that large changes in the output can be effected by varying both i and j together: in other words, there is synergy in modifying both parameters that is greater than the sum of their respective effects on the output.

Simulations using OnGuard were performed on the model described previously for the Arabidopsis (*Arabidopsis thaliana*) guard cell (Wang et al., 2012; Blatt et al., 2014; Minguet-Parramona et al., 2016) over the standard diurnal period, but with two changes. First, we incorporated step changes in light intensity instead of ramped intensity variations. Second, we introduced descriptors for light quality, dividing the incident light between red and blue spectral components, and we assigned to blue light control of the various ATPases that previously had been conferred to the total incident light. Using step changes in light intensity simplified the analysis. Incorporating the spectral definitions brings the OnGuard platform into alignment with current knowledge of the actions of light, especially of blue light, on the H^+-ATPases (Takemiya et al., 2013; Wang et al., 2014b; Yamauchi et al., 2016) and will allow future refinements in model design, but it had no material effect on model output in our formulation.

For Sobol sensitivity analysis, we stepped the light intensity from 0 to 1,000 μmol m^{-2} s^{-1} at the start of the daylight period using a mixture of 900 μmol m^{-2} s^{-1} red light and 100 μmol m^{-2} s^{-1} blue light, and we stepped the light back to 0 μmol m^{-2} s^{-1} at the end of the daylight period. All other environmental conditions were kept constant as described previously (Wang et al., 2012). A subset of 15 of the 22 transporters at the plasma membrane and tonoplast, all contributing to Ca^{2+} transport or subject to regulation by $[Ca^{2+}]_i$ in the model, was chosen to assess their impact on emergent properties in stomatal control. These transporters and their parameters are identified in an accompanying review (Jezek and Blatt, 2017) and the original descriptions of the OnGuard platform (Chen et al., 2012; Hills et al., 2012). The transporters were reflected in 45 parameters comprising, for each transporter, the transporter number, the dissociation constant, and the Hill coefficient with reference to the Ca^{2+} ligand. The parameters were varied over a range of ±20% of their default values. Efficient Monte-Carlo sampling using a Sobol sequence (Sobol, 2001; Tissot and Prieur, 2015) was used to generate parameter combinations that cover evenly the mathematical space associated with the individual parameters. In keeping with standard Sobol analysis, desired parameter ranges were scaled to the unit interval (0–1) for sampling and then rescaled to run through the model. The result was a total of 188,498 parameter combinations to test independently within OnGuard. Simulations were conducted in parallel on an in-house computer cluster. In each instance, we extracted system outputs for seven separate variables: minimum and maximum stomatal aperture, initial rates of stomatal opening and closing, the amplitude of $[Ca^{2+}]_i$ oscillations, their median periodicity, and the total number associated with stomatal closure (Minguet-Parramona et al., 2016).

Global sensitivity analysis was performed against the variance in these outputs as well as other first-order outputs derivable from them, such as the dynamic range in stomatal aperture. The analysis was performed using the R function sobolroalhs from the sensitivity package. This function implements the estimation of the Sobol sensitivity indices introduced by Tissot and Prieur (2015) using two Orthogonal Array-Based Latin Hypercubes, which allows the estimation of all closed second-order indices containing the sum of the second-order effect between two inputs and the individual effects of each input. Such analysis yields indexed values that vary in direct relation to the importance of the sensitivity of the model to the corresponding parameters. In general, Sobol index values should be positive, with a sum equal to 1, and are considered significant when the lower edge of the confidence interval is above 0 and the value itself is above 0.05 (5% risk of a zero parameter value). The code for calculating the Sobol sensitivity indices with OnGuard is available from www.psrg.org.uk.

Supplemental Data

The following supplemental materials are available.

Supplemental Appendix S1. Core OnGuard model parameters in modeling.

Received February 10, 2017; accepted April 20, 2017; published April 21, 2017.

LITERATURE CITED

Allen GJ, Chu SP, Harrington CL, Schumacher K, Hoffmann T, Tang YY, Grill E, Schroeder JI (2001) A defined range of guard cell calcium oscillation parameters encodes stomatal movements. Nature **411:** 1053–1057

Blatt MR (2000) Cellular signaling and volume control in stomatal movements in plants. Annu Rev Cell Dev Biol **16:** 221–241

Blatt MR, Armstrong F (1993) K^+ channels of stomatal guard cells: abscisic acid-evoked control of the outward rectifier mediated by cytoplasmic pH. Planta **191:** 330–341

Blatt MR, Thiel G, Trentham DR (1990) Reversible inactivation of K^+ channels of Vicia stomatal guard cells following the photolysis of caged inositol 1,4,5-trisphosphate. Nature **346:** 766–769

Blatt MR, Wang Y, Leonhardt N, Hills A (2014) Exploring emergent properties in cellular homeostasis using OnGuard to model K^+ and other ion transport in guard cells. J Plant Physiol **171:** 770–778

Chen ZH, Hills A, Bätz U, Amtmann A, Lew VL, Blatt MR (2012) Systems dynamic modeling of the stomatal guard cell predicts emergent behaviors in transport, signaling, and volume control. Plant Physiol **159:** 1235–1251

Chen ZH, Hills A, Lim CK, Blatt MR (2010) Dynamic regulation of guard cell anion channels by cytosolic free Ca^{2+} concentration and protein phosphorylation. Plant J **61:** 816–825

Dietrich P, Hedrich R (1998) Anions permeate and gate GCAC1, a voltage-dependent guard cell anion channel. Plant J **15:** 479–487

Fricker MD, Gilroy S, Read ND, Trewavas AJ (1991) Visualisation and measurement of the calcium message in guard cells. *In* W Schuch, G Jenkins, eds, Molecular Biology of Plant Development, **Vol 1**. Cambridge University Press, Cambridge, UK, pp 177–190

Gobert A, Isayenkov S, Voelker C, Czempinski K, Maathuis FJM (2007) The two-pore channel TPK1 gene encodes the vacuolar K^+ conductance and plays a role in K^+ homeostasis. Proc Natl Acad Sci USA **104:** 10726–10731

Grabov A, Blatt MR (1998) Membrane voltage initiates Ca^{2+} waves and potentiates Ca^{2+} increases with abscisic acid in stomatal guard cells. Proc Natl Acad Sci USA **95:** 4778–4783

Grabov A, Blatt MR (1999) A steep dependence of inward-rectifying potassium channels on cytosolic free calcium concentration increase evoked by hyperpolarization in guard cells. Plant Physiol **119:** 277–288

Gradmann D, Blatt MR, Thiel G (1993) Electrocoupling of ion transporters in plants. J Membr Biol **136:** 327–332

Hetherington AM, Brownlee C (2004) The generation of Ca^{2+} signals in plants. Annu Rev Plant Biol **55:** 401–427

Hills A, Chen ZH, Amtmann A, Blatt MR, Lew VL (2012) OnGuard, a computational platform for quantitative kinetic modeling of guard cell physiology. Plant Physiol **159:** 1026–1042

Jezek M, Blatt MR (2017) Integrating guard cell membrane transport for enhanced stomatal response. Plant Physiol **174:** 487–519

Keller BU, Hedrich R, Raschke K (1989) Voltage-dependent anion channels in the plasma membrane of guard cells. Nature **341:** 450–453

Kim TH, Böhmer M, Hu H, Nishimura N, Schroeder JI (2010) Guard cell signal transduction network: advances in understanding abscisic acid, CO_2, and Ca^{2+} signaling. Annu Rev Plant Biol **61:** 561–591

Lawson T, Blatt MR (2014) Stomatal size, speed, and responsiveness impact on photosynthesis and water use efficiency. Plant Physiol **164:** 1556–1570

Lemtiri-Chlieh F, MacRobbie EAC (1994) Role of calcium in the modulation of Vicia guard cell potassium channels by abscisic acid: a patch-clamp study. J Membr Biol **137:** 99–107

McAinsh MR, Brownlee C, Hetherington AM (1990) Abscisic acid-induced elevation of guard cell cytosolic Ca^{2+} precedes stomatal closure. Nature **343:** 186–188

McAinsh MR, Webb A, Taylor JE, Hetherington AM (1995) Stimulus-induced oscillations in guard cell cytosolic free calcium. Plant Cell **7:** 1207–1219

Merlot S, Leonhardt N, Fenzi F, Valon C, Costa M, Piette L, Vavasseur A, Genty B, Boivin K, Müller A, et al (2007) Constitutive activation of a plasma membrane H^+-ATPase prevents abscisic acid-mediated stomatal closure. EMBO J **26:** 3216–3226

Meyer S, Mumm P, Imes D, Endler A, Weder B, Al-Rasheid KAS, Geiger D, Marten I, Martinoia E, Hedrich R (2010) AtALMT12 represents an R-type anion channel required for stomatal movement in Arabidopsis guard cells. Plant J **63:** 1054–1062

Minguet-Parramona C, Wang Y, Hills A, Vialet-Chabrand S, Griffiths H, Rogers S, Lawson T, Lew VL, Blatt MR (2016) An optimal frequency in Ca^{2+} oscillations for stomatal closure is an emergent property of ion transport in guard cells. Plant Physiol **170:** 33–42

Novikoff AB (1945) The concept of integrative levels and biology. Science **101:** 209–215

Roelfsema MR, Hedrich R (2010) Making sense out of Ca^{2+} signals: their role in regulating stomatal movements. Plant Cell Environ **33:** 305–321

Sobol IM (2001) Global sensitivity indices for nonlinear mathematical models and their Monte Carlo estimates. Math Comput Simul **55:** 271–280

Takemiya A, Sugiyama N, Fujimoto H, Tsutsumi T, Yamauchi S, Hiyama A, Tada Y, Christie JM, Shimazaki K (2013) Phosphorylation of BLUS1 kinase by phototropins is a primary step in stomatal opening. Nat Commun **4:** 2094

Thiel G, MacRobbie EAC, Blatt MR (1992) Membrane transport in stomatal guard cells: the importance of voltage control. J Membr Biol **126:** 1–18

Tissot JY, Prieur C (2015) A randomized orthogonal array-based procedure for the estimation of first- and second-order Sobol indices. J Stat Comput Simul **85:** 1358–1381

Wang Y, Hills A, Blatt MR (2014a) Systems analysis of guard cell membrane transport for enhanced stomatal dynamics and water use efficiency. Plant Physiol **164:** 1593–1599

Wang Y, Noguchi K, Ono N, Inoue S, Terashima I, Kinoshita T (2014b) Overexpression of plasma membrane H^+-ATPase in guard cells promotes light-induced stomatal opening and enhances plant growth. Proc Natl Acad Sci USA **111:** 533–538

Wang Y, Papanatsiou M, Eisenach C, Karnik R, Williams M, Hills A, Lew VL, Blatt MR (2012) Systems dynamic modeling of a guard cell Cl^- channel mutant uncovers an emergent homeostatic network regulating stomatal transpiration. Plant Physiol **160:** 1956–1967

Yamauchi S, Takemiya A, Sakamoto T, Kurata T, Tsutsumi T, Kinoshita T, Shimazaki K (2016) The plasma membrane H^+-ATPase AHA1 plays a major role in stomatal opening in response to blue light. Plant Physiol **171:** 2731–2743